THE UNIQUE CASE OF TIN(II) FLUORIDE CONTAINING UNEXPECTED SUBSTITUTIONAL SOLID SOLUTIONS: LOCAL STRUCTURE VERSUS GLOBAL STRUCTURE

GEORGES DÉNÈS, ABDUALHAFED MUNTASAR, M. CECILIA MADAMBA & ZHIMENG ZHU
Department of Chemistry and Biochemistry, Concordia University, Canada

ABSTRACT

Solid solutions provide the means of tailoring the properties of materials by adjusting their chemical composition without phase demixing. A *solid solution* is a compound with a variable composition. *Substitutional solid solutions* are formed by replacing some atoms/ions by other atoms/ions. In order to be energetically favored, this replacement is possible only if certain criteria are met: (1) *size criterion*: there should be no more than 15% difference between the radius of the atoms/ions that are replacing each other, and (2) *bonding type criterion*: the replacing atom/ion should be able to accept the bonding type of the host. If these criteria are not met, the substitution will create an unacceptable level of stress at and around the substitution sites. In our studies of the SnF_2/MF_2 systems, where (M = Ca, Sr, Ba or Pb), we have found a $M_{1-x}Sn_xF_2$ solid solution for M = Ca and Pb, with a wide range of composition in the case of Pb. In addition, the investigation of the $SnF_2/MF_2/MCl_2$ systems revealed an even more complicated type of solid solution. All should be forbidden according to accepted criteria: the alkaline earth metal fluorides and chlorides have ionic structures, while SnF_2 has three allotropes, all which are characterized by strongly covalent bonding with a significant amount of polymerization. In addition, the similar size criterion is grossly violated, Sn^{2+} being much smaller than the alkaline earth metal, well beyond the accepted limit of about 15% for ion substitution. Furthermore, the wider solid solutions are formed with PbF_2 and BaClF, i.e. for the cations that have the largest size difference. The $Ba_{1-x}Sn_xCl_{1+y}F_{1-y}$ solid solution is by far the most unusual, and it is probably unique since it is a doubly disordered solid solution (simultaneous disorder on the cationic sita and on the anionic sites). The combined use of X-ray diffraction and Mössbauer spectroscopy was necessary in order to understand these solid solutions.
Keywords: solid solutions, divalent tin, lone pair stereoactivity, X-ray diffraction, Mössbauer spectroscopy.

1 INTRODUCTION

Compounds are defined as being matter with a constant composition each. When single phase matter has a variable composition, it is called a homogeneous solution. While the name "solution" is usually used for liquids, the tremendous development of solid state chemistry in the past half a century has given rise to solid solutions, i.e. single phase solids with a variable composition. The synthesis of solid solutions has opened the way to generate large changes in the physical properties of solid materials. For example, minute doping with an appropriate element changes insulator to semiconductors (defect semiconductivity) while much larger appropriate modifications of the chemical composition can change some insulators or moderate ionic conductors to superionics. The fluorite type (CaF_2 type) are the highest performance fluoride-ion conductors MF_2 fluorides, $\beta-PbF_2$ being the best [1]. The conductivity of the fluorite-type BaF_2 and $\beta-PbF_2$ is enhanced by about three orders of magnitude by substituting half of Ba or Pb by Sn, tin, to give $BaSnF_4$ and $PbSnF_4$ [2]–[5]. Compounds with such highly abnormal ionic conductivity at moderately high temperature, or even at ambient temperature or below, are referred to as having *superionic* properties. Among those, one finds solid solutions too, containing divalent tin and having the fluorite-type structure, such as the $Pb_{1-x}Sn_xF_2$, that has a very wide range of composition

($0 \leq x \leq 0.50$) [6], [7]. Substitution of the other metal by divalent tin can result in the formation of stoichiometric compounds that are closely related to the fluorite-type structure, such as $MSnF_4$ (M = Sr, Ba & Pb) [8], $PbSn_4F_{10}$ [9], or $CaSn_2F_6$ [10]. In contrast, some are non-stoichiometric solid solutions, such as $Pb_{1-x}Sn_xF_2$ [11], $Ca_{1-x}Sn_xF_2$ [12], or the $Ba_{1-x}Sn_xCl_{1+x}F_{1-x}$ solid solution, with disorder on the cation and the anion sites [13]. In addition to the crystal structure being closely related to the fluorite-type, therefore containing Frenkel defects with vacant sites able to lodge a fluoride ion interstitial, the presence of tin(II) or the soft ion Pb^{2+} substituting some of the other metal is essential in order to achieve high performance fluoride ion conductivity [14]. Surprisingly, even molecular SnF_2 shows a substantial fluoride ion conductivity. with $\alpha-SnF_2$ being a better conductor than $\beta-PbF_2$, the best conductor among the fluorite type MF_2 compounds [15]. The ability of covalently bonded tin(II) to fit in very large amounts in the typically ionic fluorite structure is surprising from a structural point of view. Probably even more surprising, is the fact that the presence of tin increases very substantially the fluoride ion conductivity of when one would rather expect it to decrease since tin(II) should lock a large number of fluorine atoms in non-mobile positions by forming Sn-F covalent bonds. The purpose of this work was to provide some logical scientific explanation to how the solid solutions studied here can exist despite violating the usual rules for forming solid solutions. The same problem can occur for substituting any hard-spherical cation by an element that a lone pair (Ga(I), In(I), Sn(II), Pb(II), Sb(III) or Bi(III)).

2 THEORETICAL BACKGROUND

2.1 Crystal structures

Fig. 1 shows the relationship between the crystal structure of BaF_2 and those of BaClF and $BaSnF_4$. In unsubstituted BaF_2 (Fig. 2(b)), the crystal system is cubic and the Ba^{2+} ions are in cubic $[MF_8]$ coordination, however half of the cubes of fluorides ions do not contain any metal ions and are therefore vacant $[\Upsilon F_8]$, where Υ is a metal ion vacancy. The structure of BaClF (Fig. 1(a)) is obtained from the structure of BaF_2 (Fig. 1(b)) by ordering fluoride and chloride ions according to a F-Cl sequence, parallel to the c axis of the unit-cell. This results in a tetragonal distortion with a large increase of the c unit-cell parameter, however, there is no superstructure.
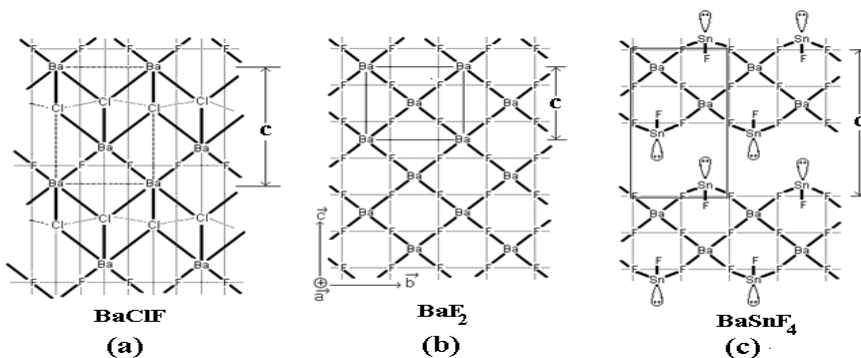

Figure 1: Projection of the structures of (a) BaClF (F-Cl order); (b) Unsubstituted BaF_2; and (c) $BaSnF_4$ (Ba-Ba-Sn-Sn order), all in the system of axes of BaF_2.

   The structure of BaSnF$_4$ (Fig. 1(c)) also results from that of BaF$_2$ by ordering barium and tin according to the Ba-Ba-Sn-Sn sequence. This results in superstructure whereby the *c* unit-cell parameter is doubled. There is also a 45° rotation of the *a* and *b* axes around the *c* axis for BaClF and BaSnF$_4$, relative to the BaF$_2$ axes, such that the unit-cell axis system, that is *a*, *b*, *c* in BaF$_2$, is *a√2/2, a√2/2, c* in BaClF and *a√2/2,* a*√2/2, 2c* in BaSnF$_4$. While the BaF$_2$ and BaClF structures can be considered to be fully ionic, this is not the case for BaSnF$_4$, where the Sn−F bonds (2.029 Å) are significantly shorter than the sum of the ionic radii (2.30 Å), thereby showing a large amount of covalency [16], [17]. The large amount of covalency of the Sn−F bonds is observed in about all of the tin(II) fluoride containing compounds. For example, this is the case for the three phases of SnF$_2$, where the shortest Sn−F bonds are clearly very short (2.048 and 2.057 Å) and show that bonding is covalent [18]–[20]. It can be seen on Fig. 1 that ionically bonded Ba^{2+} ions in the three structures form bonds to the anions from all around as can be expected for ionic bonding, whereas in BaSnF$_4$, covalent Sn-F bonds are observed only on one side of tin, while on the other side, there a non-bonding orbital containing two electrons. Such an orbital containing a non-bonded pair of electrons is called a *lone pair*. Since it is unshared, a lone pair reduces the coordination number, usually by one, two or three, and in addition, it occupies more room in the valence shell of tin, resulting in further distortion of the polyhedron of coordination. The *valence Shell Electron Pair Repulsion (VSPER)* model of Gillespie and Nyholm provides a rationale for the electron pair geometry and molecular geometry in free polyhedra (monomeric species in the gas phase, and often in liquids and solutions) [21]. Two other models, based on VSEPR, were published later in order to account for the coordination of the elements of period 5 of the periodic table that has one lone pair in its valence shell (In(I), Sn(II), Sb(III), Te(IV), I(V) and Xe(VI)) in solid phases. These models are based on the fact that the r$_+$/r$_–$ ratio of ionic radii for these elements, when coordinated by fluoride or oxide ions, is such that there is room for six anions (O$^{2−}$ or F$^−$) to make the coordination octahedral. First, the model by I.D. Brown looks at the various modes of distortions of an octahedron by a lone pair: *E* model (1 anion pushed away by the lone pair, sp^{3}d^2 hybridization, octahedral electron pair geometry, square pyramidal molecular geometry), *A* model (2 anions pushed away by the lone pair, sp^{3}d hybridization, trigonal bipyramidal electron pair geometry, see-saw molecular geometry), *C* model (3 anions pushed away by the lone pair, sp^3 hybridization, tetrahedral electron pair geometry, trigonal pyramidal molecular geometry) [22]. In the other model, the Galy-Andersson model, it is shown that the lone pair in Te(IV) occupies the same space as an oxide ion or a fluoride ion, and the lone pair forms with the O^{2-} and/or F$^-$ ions form a compact polyhedron containing the central Te(IV), that is shifted towards the lone pair [23]. We showed in an earlier work that the same is true for Sn(II) fluorides, oxides and oxide fluorides [24]. It should be noted that when the lone pair reduces the coordination number and distorts the polyhedron of coordination, it is located on an axial orbital that is a hybrid orbital. Such a lone pair is said to be *stereoactive* because it changes the stereochemistry at tin. Since covalent bonding requires orbital hybridization in order to explain the shape of the polyhedra of coordination, a stereoactive lone pair is a sure indication that bonding is covalent. In contrast, when bonding is ionic, there is no orbital hybridization and the lone pair is contained in the native *5s* orbital. Since *s* orbitals are spherical, they do not distort the coordination, and for that reason, a lone pair located on a pure *s* orbital, hence unhybridized, is called a *non-stereoactive* lone pair. Therefore, a non-stereoactive lone pair will be observed each time bonding is ionic.

2.2 Crystallography and Mössbauer spectroscopy

Crystallographic methods, by use of X-ray or neutron diffraction, allows the study of the whole crystal lattice. In case of non-stoichiometric compounds, X-ray and neutron diffraction scatter an average of the scattering power of the atoms that are disordered in a given site. On the other hand, Mössbauer spectroscopy is a local probe. It is a nuclear spectroscopy, and therefore, it probes only specific nuclides, such as ^{119}Sn in this work. Therefore, by use of ^{119}Sn Mössbauer spectroscopy, we can study tin in compounds, and the way it interacts with its neighbors and with the entire solid lattice. The nuclear spins on ^{119}Sn are 1/2 in the ground state and 3/2 in the first excited state. The ground state has no quadrupole moment, therefore it remains unsplit ($|\pm 1/2>$) in the absence of a magnetic field, even if an electric field gradient (e.f.g.) is present, while the first excited state has a quadrupole moment that interacts with an e.f.g. to give rise to two sublevels, $|\pm 1/2>$ and $|\pm 3/2>$. Therefore, the resonant absorption of γ-rays by the ^{119}Sn nuclide for each tin site will give either a doublet ($|\pm 1/2> \rightarrow |\pm 1/2>$ and $|\pm 1/2> \rightarrow |\pm 3/2>$ transitions), or a singlet ($|\pm 1/2> \rightarrow |\pm 1/2>$ only), depending on whether there is an e.f.g. acting at the nucleus or not. No hyperfine magnetic field (6 lines) was observed since tin is diamagnetic in all its oxidation states, there was no transferred field in any of the compounds studied since they are diamagnetic and no external magnetic field was applied. The line position is called *isomer shift δ*, and it is a function of the amount of valence *s* density acting at the nucleus. This makes it a function of the oxidation state of tin, of the mode of bonding and of the electronegativity of the elements bonded to tin. To a lesser extent, it is also a function of temperature (*second order Doppler shift*). In Fig. 2(A), the Sn^{2+} stannous ion gives a single peak at high isomer shift (ca. 4mm/s). The line is a singlet because the lone pair is located on the native *5s* orbital that is are spherical and therefore it generate no e.f.g. The fact that the lone pair is purely *5s* makes it that its electron density is unshared and therefore there is a non-negligible amount of *5s* electron density acting at the nucleus, resulting in a high isomer shift. An e.f.g. due to lattice distortion is possible, however its effect on the spectrum is much weaker. Fig. 2(B) shows the case of tin(II) covalently bonded to fluorine.
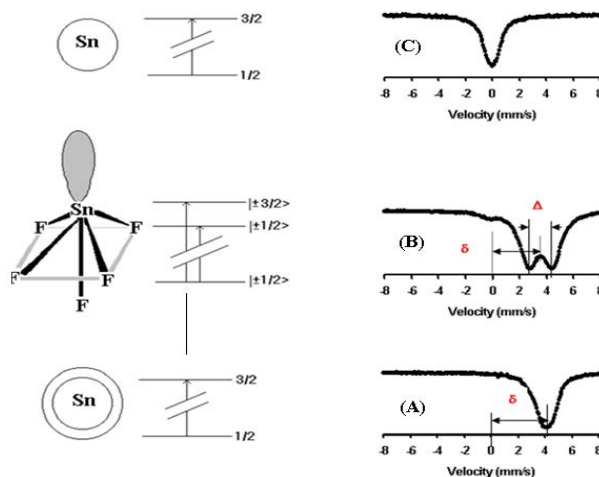

Figure 2: Mössbauer spectra for (A) Ionic Sn^{2+}; (B) Covalently bonded Sn(II) in $BaSnF_4$; and (C) $CaSnO_3$.

The stereoactive lone pair at tin generates a very large e.f.g., hence a large doublet is observed. Since the *5s* electron density is shared between the lone pair and the bonds, it is further away from the nucleus than in the case of ionic bonding, and this generates a smaller isomer shift. Fig. 2(C) is the spectrum of $CaSnO_3$. I contains Sn^{4+} ions that have completely lost their valence shell, therefore there is no more *5s* electron density acting at the nucleus. It results in a much smaller isomer shift, that is taken as reference of isomer shifts, hence 0 mm/s, since all isomer shifts are referenced to $CaSnO_3$ at ambient temperature. I gives a single line since $CaSnO_3$. has the perovskite structure where the Sn^{4+} ions are in an octahedral site.

It results from the above that the information obtained for each tin site are (i) its oxidation number, and in this study, for tin(II), (ii) the identification of the non-metal bonded to tin, (iii) the tin site distortion, and (iv) the tin type of bonding (ionic or covalent). Fig. 2 shows the influence of oxidation number and type of bonding on the Mössbauer spectrum. In addition, the lattice strength can also be estimated. Resonant absorption of γ−photons is necessary in order to produce a Mössbauer spectrum, and less and less of this occurs when temperature increases and when the lattice is weak, due to phonons. Therefore, a weak lattice will result in a weaker spectrum.

2.3 The Hume-Rothery rules of substitutional solid solutions

The Hume-Rothery rules of substitutional solid solutions were designed for alloys, however they can be extended to substitutions in ionic compounds. The rules are the following [25]:

1. The atomic radius of the solute and solvent atoms must differ by no more than 15%: this rule is violated in all cases: 17% for substituting Ca2+ by Sn2+, 35% for substituting Pb2+ by Sn2+, 25% for substituting Cl- by F-, and 25% for substituting F- by Cl-.
2. The crystal structures of solute and solvent must be similar: this rule is also violated when Sn(II) replaces Ca2+ or Pb2+ since both CaF2 and β−PbF2 have the purely ionic fluorite type structure, while the structure of the three phases of SnF2 is polymeric with covalent bonding.
3. The solute and the solvent must have the same valency: this rule is obeyed since all metals are in the same oxidation number (+2).
4. The solute and solvent should have similar electronegativity: this rule is obeyed only for replacing Pb by Sn (5% difference), however it is violated for replacing Ca by Sn (80% difference), Cl by F (33% difference) and F by Cl (25% difference).

3 MATERIAL CHARACTERIZATION

X-ray powder diffraction was carried out by use of a Philips PW1050 diffractometer that had been automated with the Sie112 Sietronics® system from Difftech. This allowed a phase identification of phases already known, by comparison with the diffraction patterns of starting materials and other possible side products already collected in our laboratory and by use of the µPDSM Micro Powder Diffraction Search Match® from Fein-Marquat. Only the phases of interest in this study were subjected to further analysis.

Electrical conductivity was measured on polycrystalline samples pressed to form a pellet, each face of which was covered with a thin layer of gold by evaporation under vacuum. The measurements were carried out under dry nitrogen in ac versus frequency (300 kHz–10 Hz)

at each temperature, and analyzed by the complex impedance method. The transport number was measurement was measured in dc using a gold blocking electrode.

The Mössbauer spectra were recorded using the following set-up. The source was a nominally 25 mCi $Ca^{119m}SnO_3$ γ−ray source from Ritverc GmbH. Isomer shifts were referenced relative to a standard $CaSnO_3$ absorber at ambient temperature. The counting system was a scintillation counter from Harshaw, equipped with a 1 mm thick (Tl)NaI crystal. A palladium foil was used to absorb the 25.04 keV and the 25.72 keV X-ray lines generated by the source decay from the 11/2 spin level of the ^{119m}Sn precursor to the 3/2 spin of the first excited state. The Doppler velocity ($\pm$ 10 mm/s) was generated by use of an Elscint driving system, including a Mössbauer MVT-4 velocity transducer, a Mössbauer MDF-N-5 waveform generator and a MFG-N-5 driver. The amplifier, the single channel analyzer and the multichannel analyzer are combined in the Tracor Northern TN7200 system. After, the data were transferred to a computer for storage and processing. Low temperature spectra were recorded using an ADP Cryogenics helium closed-cycle refrigerator equipped with a two-stage Displex®. Computer processing of the data was performed using the MOSGRAF-2009 suite [26].

4 RESULTS AND DISCUSSION

4.1 The M1−xSnxF2 solid solution (M = Ca and Pb)

The $Ca_{1-x}Sn_xF_2$ solid solution was obtained by the reaction of calcium nitrate with stannous fluoride in aqueous solution for a large molar ratio $\chi = Ca(NO_3)_2/SnF_2$ ($\chi > 0.65$). When the reaction mixture contains a large excess of SnF_2, crystalline $CaSn_2F_6$ is obtained, while at medium ratios, a mixture of $CaSn_2F_6$ and the $Ca_{1-x}Sn_xF_2$ solid solution precipitates, and the pure solid solution is obtained only at a larger excess of calcium nitrate (Fig. 3). The $Ca_{1-x}Sn_xF_2$ solid solution can also be prepared by stirring in water $CaSn_2F_6$ or the mixture of $CaSn_2F_6$ and the $Ca_{1-x}Sn_xF_2$ solid solution.

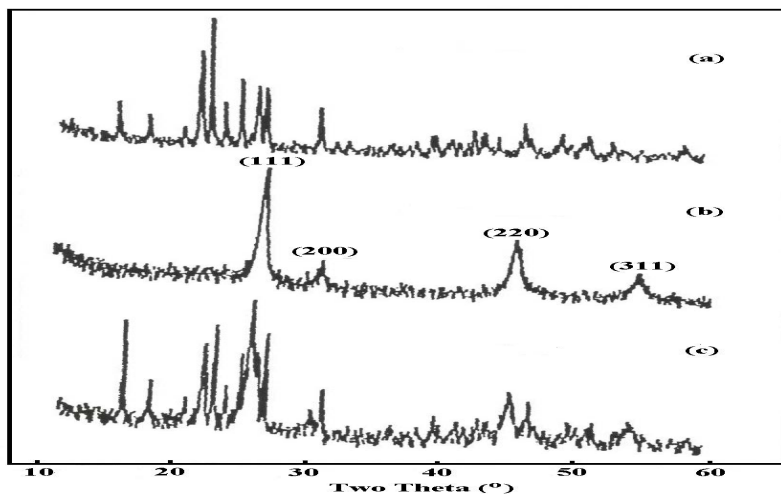Figure 3: X-ray powder diffraction pattern of the precipitate obtained versus the molar fraction χ of $Ca(NO_3)_2$(aq) added to a solution of SnF_2: (a) $\chi = 0.09$: $CaSn_2F_6$; (b) $\chi = 0.66$: $Ca_{1-x}Sn_xF_2$ ($x \approx 0.30$); (c) $\chi = 0.43$: a mixture of $CaSn_2F_6$ and $Ca_{1-x}Sn_xF_2$.

It was found that $CaSn_2F_6$ decomposes by leaching in water to give the mixture of phases, and finally the pure $Ca_{1-x}Sn_xF_2$ solid solution, provided enough water is used and the stirring time is sufficient. Elemental analysis by Atomic Absorption Spectroscopy (AAS) showed that between a quarter and a third of the calcium is replaced by tin ($0.25 < x < 0.34$). It can be seen on Fig. 3(b) that the X-ray diffraction pattern of the $Ca_{1-x}Sn_xF_2$ solid solution indexes in the same face centered cubic (fcc) lattice as CaF_2, with no measurable change of unit-cell parameter ($a \approx 5.463$ Å) (Fig. 4(a)). In addition, the Bragg peaks are very significantly broadened. For visualizing the broadening, one can compare the width of the (111) peak of $Ca_{1-x}Sn_xF_2$ to the peaks of $CaSn_2F_6$ at a similar angle (Fig. 3), or to CaF_2 (Fig. 4(a)). The peaks of $CaSn_2F_6$ and those of CaF_2 are not broadened, while the broadening for $Ca_{1-x}Sn_xF_2$ shows that the material is nanocrystalline. This is confirmed by calculating the average crystallite diameter from the line broadening, by the Scherrer method, after Warren's correction for instrumental broadening [27]. The average crystallite diameter was found to be ≈ 90 Å. The $Pb_{1-x}Sn_xF_2$ solid solution was obtained by the reaction of appropriate amounts of PbF_2 and SnF_2 in dry conditions at 500ºC in sealed copper tubes under a dry nitrogen atmosphere, according to a method described by one of us (GD) [28]. After an overnight heating, the tubes were taken out of the furnace and allowed to cool to ambient temperature. X-ray powder diffraction of $Pb_{1-x}Sn_xF_2$ showed the diffraction pattern of a cubic unit-cell for $0 < x < 0.30$, similar to that of β−PbF_2, i.e. fluorite -type, like for the $Ca_{1-x}Sn_xF_2$ solid solution. The solid solution continues all the way to $x = 0.50$. The limit at $x = 0.50$ is β−$PbSnF_4$. However, for $x > 0.30$, a β−$PbSnF_4$ type of tetragonal distortion ($c < a$) is present, starting from 0 at $x = 0.30$, and increasing with increasing x. Both solid solutions are fluoride ion conductors. The conductivity of $Pb_{1-x}Sn_xF_2$ was found to increase up to three orders of magnitude with the tin content x, from $x = 0$ (β−PbF_2) to $x = 0.50$ (β−$PbSnF_4$). This was attributed to an increasing number of defects created by the substitution of Pb by Sn [29]. On the other hand, the conductivity of $Ca_{1-x}Sn_xF_2$ was measured to be much lower, in between that of CaF_2 and that of SnF_2. This is likely due to the smaller size of the Ca^{2+} ion, compared to Pb^{2+}, that makes the pathway available for the fluoride motion be smaller, probably barely large enough for the diffusion of fluoride ions. The main interest of this report is to discuss the coordination of tin in the two cubic solid solutions. The cubic symmetry of the unit-cell, with the fluorite type structure, together with the absence of lattice distortion and of a superstructure, makes it that Sn and Ca or Pb are fully disordered on the metal ion site of the lattice. The cubic symmetry of the site implies that the tin(II) lone pair has to be non-stereoactive, i.e. that Sn-F bonding is ionic and there should be no site distortion. However, Sn(II)-F bonding is always found to be covalent. The bonding type and stereoactivity of the lone pair can be established by Mössbauer spectroscopy. The spectrum of $Ca_{1-x}Sn_xF_2$ (Fig. 4(c-2)) is a large quadrupole doublet, like that of $BaSnF_4$ (Fig. 2(B)), and this is characteristic of a highly stereoactive lone pair. Now, we are faced with a contradiction between the conclusions of X-ray diffraction (Sn is in cubic coordination with ionic bonding and a non-stereoactive lone pair) and those of Mössbauer spectroscopy (Sn is in a highly distorted site due to a stereoactive lone pair, and bonding is covalent).

The contradictory results can be reconciled if Sn is shifted out of the center of its F_8 cubic site to give room to the stereoactive lone pairs (Fig. 5). In order to keep the overall cubic symmetry of the crystal lattice, the structure must be disordered in two ways: (i) a *positional M/Sn disorder* (M = Ca or Pb) over the M site of the fluorite structure; (ii) an *orientational disorder* of the shift of Sn towards any of the six faces of the F_8 cube it occupies, with the lone pair pointing towards the opposite face of the cube. This makes tin be bonded to four fluorine atoms at the corners of a square, with tin and the lone pair being on the line normal to the center of that square. It results in five electron pairs around tin (four bonding pairs and

a lone pair), to make the electron pair geometry be square pyramidal, and the molecular geometry is also square pyramidal. This is not the geometry expected by the VSEPR model, that predicts a trigonal bipyramidal electron pair geometry for 5 electron pairs, and a see-saw molecular geometry when one of the five pairs is a lone pair. The VSEPR model is designed for free groups in the gas phase and usually in liquids. The lattice energy accounts for the difference. The same square pyramidal coordination was found to be present in SnO [30].
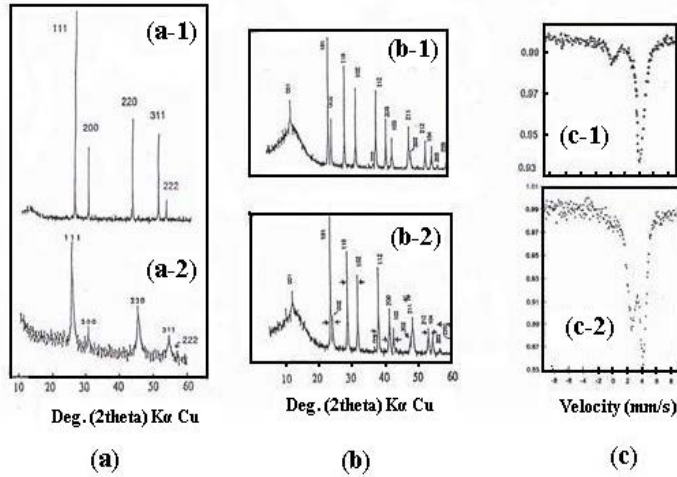

Figure 4: (a): X-ray powder diffraction pattern of (a-1) CaF2 and (a-2) of Ca1-xSnxF2 (x = 0.27); (b): X-ray powder diffraction pattern of (b-1) BaClF and (b-2) of Ba1−xSnxCl1+yF1−y (x = 0.15, y = 0.094); (c) 119Sn ambient temperature Mössbauer spectrum of: (c-1) Ca1−xSnxF2 (x = 0.27) and (c-2) Ba1−xSnxCl1+yF 1−y (x = 0.15, y = 0.094).
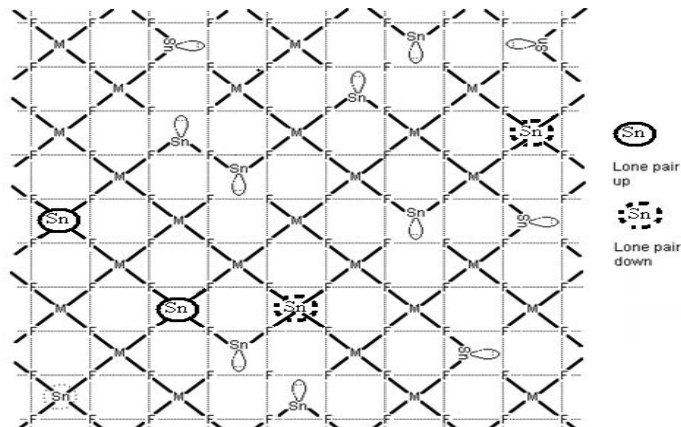

Figure 5: Projection of a structural model of the disordered M/Sn/F phases: M and Sn are randomly distributed in the $[F_8]$ cubes (*positional disorder*) the tin lone pair points randomly towards any of the six faces of the $[F_8]$ cubes (*orientational disorder*).

4.2   The Ba1−xSnxCl1+yF1-y solid solution

Reactions of $BaCl_2.2H_2O$ with SnF_2 in aqueous solutions versus the molar ratio Ba/Sn, a short for $\chi = BaCl_2.2H_2O$ / $[BaCl_2.2H_2O + SnF_2]$ gave the following precipitates, versus increasing χ, $BaSn_2F_6$ (already known), then three new phases, $BaSn_2Cl_2F_4$, $BaSnCl_3.0.8H_2O$, and the $Ba_{1-x}Sn_xCl_{1+y}F_{1-y}$ solid solution, the latter free of $BaSnCl_3.0.8H_2O$ only for $\chi > 0.87$. Elemental analysis showed that $x \approx 0.15$ and $y \approx 0.10$ in most cases. In addition, a much wider $Ba_{1-x}Sn_xCl_{1+y}F_{1-y}$ solid solution was obtained by reactions of appropriate amounts of $BaCl_2$, BaF_2 and SnF_2 in dry conditions, at 350°C under dry nitrogen, in sealed copper tubes, according to the procedure described in reference [28]. The limits of the solid solution were found to be the following: $0<x<0.25$ and $-0.15<y<0.15$. The X-ray diffraction pattern of the solid solution shows that it has the same set of Bragg peaks as for unsubstituted BaClF, with a minor peak shifts due to a small change of the tetragonal unit-cell parameters: a decreases by 0.91% and c increases by 0.97%, resulting in a shrinking of the volume by 0.86% (Fig. 4b). The lack of further lattice distortion or of superstructure peaks shows that tin has to be disordered with Ba^{2+} ions on the same site. This raises two problems. First, if tin is bonded to fluorine, it should have covalent bonding, however in order for substitution to take place, the two elements, Ba and Sn, should have the same mode of bonding, and Ba is in the form of Ba^{2+} in BaClF (Fig. 1(a)) and in all its compounds. Second, if tin is bonded to chloride ions, it could form ionic bonding, as in Ba_2SnCl_6., however Sn^{2+} ions are too small to fit tightly in the large Ba^{2+} site of the BaClF structure. Mössbauer spectroscopy can provide tell what the tin bonding type is, according to the model of spectra shown on Fig. 2. The results shows that bonding in the $Ba_{1-x}Sn_xCl_{1+y}F_{1-y}$ solid solution depends on the method of preparation. The spectrum of precipitated samples is a single line with an intensity that shows the recoil-free fraction is similar to that of other tin(II) fluorides or chlorides (Fig. 4(c-1)). In all cases, the small broad peak at ca. 0 mm/s) is that of amorphous SnO_2 due to a minor oxidation at the surface of the particles. However, the Mössbauer results of the solid solution prepared by the dry method at high temperature show a more complex bonding system (Fig. 6). When the Mössbauer spectrum is recorded at constant x ($x = 0.225$), i.e. at fixed tin content, versus y ($y = -0.15$ to $+0.25$), i.e. with decreasing amounts of fluorine and increasing amounts of chlorine, to keep the ratio metals/halogens equal to 2, a dramatic change of the Mössbauer spectrum takes place. For $y = -0.15$ (Fig. 6(a)), i.e. when the amount of fluorine is larger than that of chlorine, the spectrum is a highly asymmetric doublet, that becomes rapidly much more asymmetric as y becomes less negative, i.e. as the amount of fluorine decreases and the amount of chlorine increases. For $y = 0.10$ (Fig. 6(f)), the low velocity line has basically disappeared and the Mössbauer spectrum is now a single line. As y increases further (increase of Cl at the expense of F), the spectrum remains a single line, but the line intensity becomes very small. These changes versus y show that, when the amount of F exceeds that of Cl ($y<0$), the doublet is due to covalently bonded tin with a stereoactive lone pair. The large asymmetry of the spectrum, is due to the peak at ca. 4 mm/s attributed to ionic tin, the Sn^{2+} stannous ion, like in Fig. 2(c), and that peak overlaps with high velocity peak of the doublet. It results that the bonding of tin to the BaClF type lattice is very sensitive to the ratio Cl/[Cl+F]. When there is an excess fluorine ($y<0$), some of the tin forms covalent bonds (Fig. 7(a)), as expected for Sn-F bonds, mixed with ionic Sn^{2+}, that can be expected to bind to chloride ions. When the amount of chlorine increases at the expense of fluorine, the amount of covalently bonded tin decreases rapidly, and for $y>0$, most of the tin forms ionic bonds (Fig. 7(b)). For the highest y values, the spectrum is so weak that it is barely detectable. This shows a dramatic decrease of recoil-free fraction of the ionic tin at the highest amounts of chlorine. This can be understood by the fact that Sn^{2+} occupies the Ba^{2+} site. However, since

the ionic radius of Ba^{2+} is much larger than that of Sn^{2+}, the stannous ion occupies a site that is much oversized for it. It can therefore not forming proper bonding and it rattles in. The large thermal vibrations of tin explains the very low recoil-free fraction.
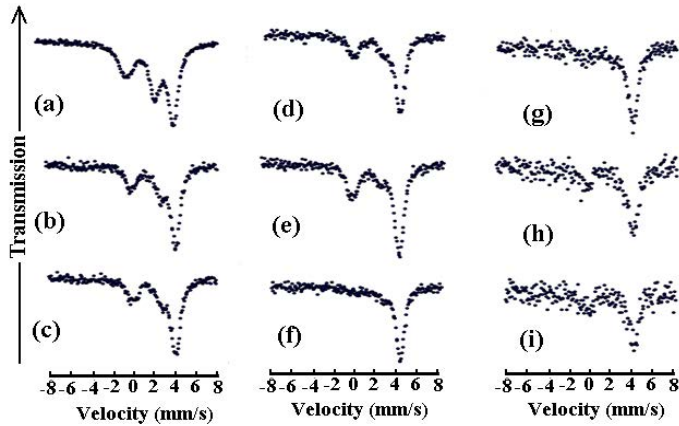

Figure 6: Ambient temperature ^{119}Sn Mössbauer spectrum of $Ba_{1-x}Sn_xCl_{1+y}F_{1-y}$ solid solution prepared by direct reaction at 350°C for 43 hours, x = 0.225, and (a): y = −0.15; (b): y = −0.10; (c): y = −0.05; (d): y = 0.00; (e): y = 0.05; (f): y = 0.10; (g): y = 0.15; (h): y = 0.20; (i): y = 0.25. All samples contain the same amount of tin, the same amount of sample was used for each, and the data of spectra for y≥0.15 were collected for 15–20 days versus only 2 or 3 days for the others.
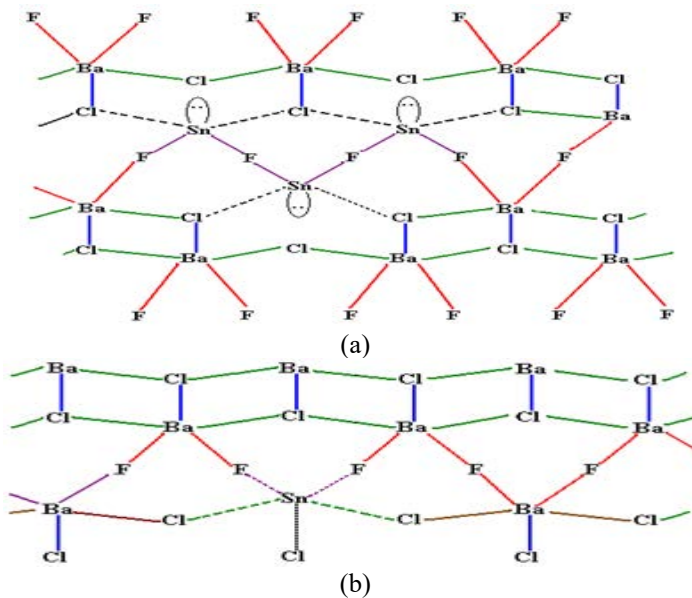

Figure 7: Model of disorder between (a) Ba^{2+} ions, Sn^{2+} ions and (b) covalently bonded Sn(II) on the Ba^{2+} site of the BaClF structure of $Ba_{1-x}Sn_xCl_{1+y}F_{1-y}$.

This was confirmed by recording a spectrum of the same sample at 17 K in order to freeze the thermal vibrations. It resulted a 35-fold increase of the intensity of the Mössbauer peak as the thermal vibrations are frozen, in contrast with a 4 fold increase after the same cooling the precipitated sample.

5 CONCLUSION

This study has shown that, even when normal rules of forming solid solutions are badly violated, one should not rule out automatically that a solid solution will not be formed. The Hume-Rothery rules of substitutional solid solutions were designed specifically for alloys. Although they work often also for ionic compounds, this is not always the case, as the present study has shown. Atoms can sometimes overcome rules, and tin(II) does it by forming covalent bonding to the fluorine of some ionic structures, if conditions are appropriate. Understanding bonding in the $M_{1-x}Sn_xF_2$ and in the $Ba_{1-x}Sn_xCl_{1+y}F_{1-y}$ solid solutions would not have been possible without the use of ^{119}Sn Mössbauer spectroscopy.

ACKNOWLEDGEMENT

REFERENCES

[1]   Fang, W. & Rapp, R.A., The electrical conductivity of β−PbF$_2$. *J. Electrochem. Soc.*, **125**(5), pp. 683–687, 1978.
[2]   Dénès, G., Birchall, T., Sayer M. & Bell M.F., BaSnF$_4$ – A new fluoride ionic conductor with the α−PbSnF$_4$. Structure. *Solid State Ionics*, **13**(3), pp. 213–219, 1984.
[3]   Dénès, G., Milova, G., Madamba, M.C. & Perfiliev, M., Structure and ionic transport of PbSnF$_4$ - superionic conductor. *Solid State Ionics*, **86**(88), pp. 77–82, 1996.
[4]   Durand-Le, F.M., Pannetier, J. & Dénès, G., Multiple sites and mobility in ionic conductors by NMR dipolar transient effects. *Phys. Rev. B,* **33**(1), pp. 632–634, 1986.
[5]   Sorokin, N.I. et al. Electrical properties of PbSnF$_4$ materials prepared by different methods. *Inorg. Mater.*, **37**(11), pp. 1178–1182, 2001.
[6]   Durand, M., Pannetier, J. & Dénès, G., Etude par R.M.N. du mouvement des fluors dans la solution solide Pb$_{0.9}$Sn$_{0.1}$F$_2$. *J. Physique*, **41**(8), pp. 831–836, 1980.
[7]   Vilminot, S., Perez, G., Granier, W. & Cot, L., High ionic conductivity in new Fluorine compounds of Tin II. II. On the binary system PbF$_2$−SnF$_2$. *Solid State Ionics*, **2**(2), pp. 91–94, 1981.
[8]   Dénès, G., Pannetier, J. & Lucas, J., Les fluorures à structure PbFCl (M = Pb, Sr, Ba). *C. R. Acad. Sc. Paris*, 2**80 C**, pp. 831–834, 1975.
[9]   Dénès, G., PbSn$_4$F$_{10}$: A new disordered fluorite-type fast ion conductor *J. Solid State Chem.*, **74**(2), pp. 343–352, 1988.
[10]   Bell, M.F., Dénès, G. & Zhu, Z., *Mater. Res. Soc. Symp. Proc.*, **756**, pp. 387–392, 2003.
[11]   Dénès, G., Yu, Y.H., Tyliszczak, T. & Hitckcock, A.P., Sn-K and Pb-L$_3$ EXAFS, X-Ray diffraction and ^{119}Sn mössbauer spectroscopic studies of ordered β−PbSnF$_4$ and disordered Pb$_{1-x}$Sn$_x$F$_2$ (x = 0.3, 0.4) solid solutions and PbSn$_4$F$_{10}$: High performance fluoride ion conductors. *J. Solid State Chem.*, **104**(2), pp. 239–252, 1993.
[12]   Dénès, G., Muntasar, A. & Zh, Z., X-Ray diffraction and mössbauer spectroscopic study of disordered Tin in the fluorite type and related structures: $M_{1-x}Sn_xF_2$ and

$Ba_{1-x}Sn_xCl_{1+y}F_{1-y}$ solid solutions and $PbSn_4F_{10}$. *Hyperf. Inter. (C)*, **1**, pp. 468–471, 1996.

[13] Dénès, G. & Muntasar, A., Bonding in the doubly disordered $Ba_{1-x}Sn_xCl_{1+y}F_{1-y}$ solid solution. *Hyperf. Inter.*, **153**(1–4), pp. 91–119, 2004.

[14] Dénès, G., Failure of the frenkel defect model to explain the trend in anionic conductivity in the MF_2 fluorite structure and related $MSnF_4$ materials. *Mater. Res. Soc. Symp. Proc.*, **369**, pp. 295–300, 1995.

[15] Ansel, D., Debuigne, J., Dénès, G., Pannetier, J. & Lucas J., About SnF_2 stannous fluoride. V: conduction characteristics. *Ber. Bunsenges. Phus. Chem.*, **82**(4), pp. 376–380, 1978.

[16] Birchall, T., Dénès, G., Ruebenbauer, K. & Pannetier, J. A neutron diffraction and [119]Sn mössbauer study of $BaSnF_4$ and $BaSnF_4$. *Hyperf. Inter.*, **29**(1–4), pp. 1331–1334, 1986.

[17] Shannon, R.D. & Prewitt, C.T., *Acta Cryst. B*, **25**, p. 725,1970.

[18] Dénès, G., Pannetier, J., Lucas, J. & Le Marouille, J.Y., About SnF_2 stannous fluoride. I. crystallochemistry of $\alpha- SnF_2$. *J. Solid State Chem.*, **30**(3), pp. 335–343, 1979.

[19] Pannetier, J., Dénès, G. & Lucas, J., About SnF_2 stannous fluoride. ii. crystal structure of β and $\gamma-SnF_2$. *J. Solid State Chem.*, **33**(1), pp. 1–11, 1980.

[20] Dénès, G., Pannetier, J., Durand, M. & Buevoz, J.L. $\beta\leftrightarrow\gamma-SnF_2$ phase transition: neutron diffraction and NMR study. *J. Physique (Paris)*, **41**(9), pp. 1019–1024, 1980.

[21] Gillespie, R.J. & Nyholm, R.S., *Quart. Rev.Chem. Soc.*, **11**, p. 339, 1957.

[22] Brown, I.D., *J. Solid State Chem.*, **11**, p. 214, 1974.

[23] Galy, J, Meunier, G., Andersson, S. & Aström, A., *J. Solid State Chem.*, **13**, p. 142, 1975.

[24] Dénès, G., Muntasar, A., Madamba, M.C. & Merazig, H. Tin(II) lone pair stereoactivity: influence on structures and properties and mössbauer spectroscopic properties. *Mössbauer Spectroscopy: Applications in Chemistry, Biology and Nanotechnology,* eds V.K. Sharma, G. Klingelhofer & T. Nishida, Wiley, 2013.

[25] Hume-Rothery, W. & Powell, H.M., *Z. Krist.,* **91**, p. 23, 1935.

[26] Ruebenbauer, K. & Duraj, Ł., www.elektron.up.krakow.pl/mosgraf-2009.

[27] Warren, B.E., *X-ray Diffraction*, ed. 2, Dover Pub: New York, pp. 251–262, 1990.

[28] Dénès, G., The "Bent Copper Tube": A new inexpensive and convenient reactor for fluorides of metals in suboxidation states. *J. Solid State Chem.*, **77**, pp. 54–59, 1988.

[29] Vilminot, S., Perez, G., Granier, W. & Cot, L., High ionic conductivity in new fluorine compounds of tin II. II. On the binary system PbF_2-SnF_2. *Solid State Ionics*, **2**(2), pp. 91–94, 1991.

[30] Pannetier, J. & Dénès, G., Tin(II) oxide: structure refinement and thermal expansion. *Acta Cryst. B* **36**, pp. 2763–2765, 1980.